© American Society for Mass Spectrometry, 2016

J. Am. Soc. Mass Spectrom. (2017) 28:136–144
DOI: 10.1007/s13361-016-1501-2

RESEARCH ARTICLE

Absolute Quantification of Rifampicin by MALDI Imaging Mass Spectrometry Using Multiple TOF/TOF Events in a Single Laser Shot

Boone M. Prentice,[1,4] Chad W. Chumbley,[2,4] Richard M. Caprioli[1,2,3,4]

[1]Department of Biochemistry, Vanderbilt University, 9160 MRB III, Nashville, TN 37232, USA
[2]Department of Chemistry, Nashville, TN 37232, USA
[3]Departments of Pharmacology and Medicine, Nashville, TN 37232, USA
[4]Mass Spectrometry Research Center, Nashville, TN 37232, USA

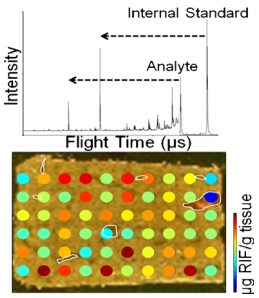

Abstract. Matrix-assisted laser desorption/ionization imaging mass spectrometry (MALDI IMS) allows for the visualization of molecular distributions within tissue sections. While providing excellent molecular specificity and spatial information, absolute quantification by MALDI IMS remains challenging. Especially in the low molecular weight region of the spectrum, analysis is complicated by matrix interferences and ionization suppression. Though tandem mass spectrometry (MS/MS) can be used to ensure chemical specificity and improve sensitivity by eliminating chemical noise, typical MALDI MS/MS modalities only scan for a single MS/MS event per laser shot. Herein, we describe TOF/TOF instrumentation that enables multiple fragmentation events to be performed in a single laser shot, allowing the intensity of the analyte to be referenced to the intensity of the internal standard in each laser shot while maintaining the benefits of MS/MS. This approach is illustrated by the quantitative analyses of rifampicin (RIF), an antibiotic used to treat tuberculosis, in pooled human plasma using rifapentine (RPT) as an internal standard. The results show greater than 4-fold improvements in relative standard deviation as well as improved coefficients of determination (R^2) and accuracy (>93% quality controls, <9% relative errors). This technology is used as an imaging modality to measure absolute RIF concentrations in liver tissue from an animal dosed in vivo. Each microspot in the quantitative image measures the local RIF concentration in the tissue section, providing absolute pixel-to-pixel quantification from different tissue microenvironments. The average concentration determined by IMS is in agreement with the concentration determined by HPLC-MS/MS, showing a percent difference of 10.6%.

Keywords: Imaging mass spectrometry, TOF/TOF, Tandem mass spectrometry, MS/MS, Rifampicin, Multiplexed

Received: 10 May 2016/Revised: 31 August 2016/Accepted: 2 September 2016/Published Online: 21 September 2016

Introduction

Matrix-assisted laser desorption/ionization imaging mass spectrometry (MALDI IMS) technology can measure the distribution of compounds within tissue sections [1, 2]. Increasingly, MALDI IMS is used in the pharmaceutical industry to measure the distributions of therapeutic agents and their metabolites in tissue specimens [3]. Classic analytical approaches such as autoradiography [4, 5] and tissue homogenate LC-MS [6–8] analysis have been used extensively in drug and metabolite characterizations; however, these often provide an incomplete analysis. For example, though autoradiography provides a quantitative measure of localization, it often lacks the molecular specificity to distinguish between a drug and its metabolites. Homogenate LC-MS offers a quantitative approach with the required molecular specificity to easily distinguish between a drug and its metabolites, but lacks a spatial component to the analysis. MALDI IMS offers both the required spatial dimension and molecular specificity, which are important for analyzing pharmacology, pharmacokinetics, transport, and metabolism.

Electronic supplementary material The online version of this article (doi:10.1007/s13361-016-1501-2) contains supplementary material, which is available to authorized users.

Correspondence to: Richard M. Caprioli;
e-mail: richard.m.caprioli@vanderbilt.edu

Several recent reports highlight the potential for quantitative MALDI IMS [9–15]. For example, the creation of a synthetically dosed tissue homogenate model allows for the quantitative comparison to a tissue section dosed in vivo [16, 17]. This requires preparing a tissue homogenate spiked with different concentrations of the drug for each tissue microenvironment (e.g., medulla and cortex of the kidney). Extinction coefficients have also been used to quantify each analyte in microenvironments of the tissue [18]. However, absolute quantification by MALDI IMS remains challenging due to matrix coating heterogeneity, tissue heterogeneity, poor analyte extraction, and ionization suppression effects [19]. Internal standards have been used in the bulk analysis of tissue sections in order to correct for some of these concerns [18, 20–31]. Recently, we have reported the use of an isotopically labeled internal standard for pixel-to-pixel quantification [32]. In this method, a standard calibration curve is prepared on an adjacent, non-dosed tissue section. An isotopically labeled internal standard is then used to compare the ion intensity from the calibration curve with that from the dosed tissue section and allows for the quantification of tissue microenvironments.

The analysis of low molecular weight analytes, such as drugs and metabolites, can be complicated by the vast excess of MALDI matrix background signal present in this region of the mass spectrum [33, 34]. Our recent quantitative MALDI IMS method leveraged the power of tandem mass spectrometry (MS/MS) to provide the required sensitivity and molecular specificity [32]. Most quantitative MS/MS experiments rely on the use of isotopically labeled internal standards to perform the analysis in one of two ways: by broadening the MS/MS isolation window so as to pass both the analyte and internal standard ions [22, 23, 27, 32, 35, 36] or by using multiple isolation windows to isolate ions of disparate *m/z* [37, 38]. We have recently utilized a high-speed TOF/TOF system to perform multiple isolation events in a single laser shot for quantitative MALDI MS/MS analyses of drugs in pooled human plasma [39].

Herein, we demonstrate the application of multiple TOF/TOF events in the same laser shot for quantitative MALDI IMS. We first validate the quantitative nature of this approach by performing quantitative MALDI analysis of spotted samples of human plasma containing the drug rifampicin (RIF). We then extend this methodology to the in vivo IMS analysis of RIF in rabbit liver, the results of which are shown to agree well with data from homogenate LC-MS/MS. By performing multiple TOF/TOF events in the same laser shot, we are able to reference the analyte signal intensity to that of the internal standard in each laser shot even when the analyte and internal standard are disparate in *m/z*. For these studies, rifapentine (RPT), an analogue of RIF that differs in mass by ~56 Da, is used as an internal standard. In this experiment, simply broadening the isolation window would pass an excess of chemical noise, impairing quantification. With this TOF/TOF approach, we demonstrate accurate pixel-to-pixel IMS quantification while maintaining sensitivity and chemical specificity.

Experimental

Materials

Standard RIF, RPT, and 2,4,6-trihydroxyacetophenone (THAP) were obtained from Sigma-Aldrich (St. Louis, MO, USA). Ethanol (200 proof) was acquired from Pharco-AAPER (Brookfield, CT, USA), and 18 MΩ water was obtained from a Milli-Q water purification system (Millipore, Billerica, MA, USA). Pooled normal human plasma was purchased from Innovative Research (Novi, MI, USA). Isotopically labeled $^{13}C_1$,$^{2}H_1$-RIF was synthesized as described previously [32].

Sample Preparation

Stock solutions of RIF (7.36 mg/mL) and RPT (0.566 mg/mL) were prepared in 95% ethanol and stored at –80 °C. Working calibration solutions of RIF (0.700–100.0 μM) included 50.0 μM RPT as an internal standard and a final concentration of 30% pooled human plasma containing K2EDTA as an anticoagulant. Concentrations below the LOQ (3.00 μM) have been omitted from the figures for simplicity. The total volume of each solution was 50.0 μL. A quality control (QC) solution of 50.0 μM RIF with 50.0 μM RPT in 30% plasma was also included in the analysis. The solutions were premixed 1:1 with 50 mg/mL THAP in 95% ethanol and manually spotted (0.500 μL twice for a total volume of 1.00 μL) onto a gold-coated stainless steel target for analysis. Calibration curves were spotted seven times and then analyzed, with five of the analyses included in quantitative calculations based on accuracy (passing QC), spot homogeneity and quality, and successful instrument data acquisition.

In vivo IMS was performed on liver from a New Zealand white rabbit infected with *Mycobacterium tuberculosis* that was orally administered a cocktail of pharmaceuticals (rifampicin/isoniazid/pyrazinamide/moxifloxacin at 30/50/125/25 mg/kg) once per day for 7 d and sacrificed 4 h and 21 min after the final dose (with the approval of the institutional animal care and use committee of the NIH/NIAID) [32, 40–42] The tissue was disinfected via irradiation with UV light, flash-frozen, and stored at 80 °C until analysis. The specimen was sectioned at 12 μm thickness on a cryostat and thaw-mounted onto a gold-coated stainless steel target. A 12 μm thick section of a liver not dosed with RIF was also thaw-mounted onto the target for deposition of the calibration curve microspots. A serial section was stained with H&E for histologic comparisons. A calibration curve of RIF (0–24.0 μM RIF with 20.0 μM RPT) was deposited onto the non-dosed control liver tissue section using eight passes of five droplets each with a robotic spotter (Portrait 630; Labcyte, Sunnyvale, CA, USA). A QC solution (14 μM RIF with 20 μM RPT) was also deposited onto the non-dosed section. The internal standard was deposited in a microspotted array with a 1 mm spatial resolution across the tissue dosed in vivo. The matrix (20 mg/mL THAP in 50% ethanol/water) was deposited onto the calibration standard and dosed tissue microspots using four passes of 100 droplets each.

The average spot diameter was measured to be approximately 590 ± 52 μm.

TOF/TOF Mass Spectrometry

Experiments were performed on a MALDI TOF/TOF mass spectrometer (300 Tandem; SimulTOF Systems, Sudbury, MA, USA) equipped with a 349 nm, diode-pumped, frequency-tripled Nd:YLF laser capable of laser repetition rates up to 5 kHz (Spectra-Physics, Santa Clara, CA, USA) [34, 39]. A laser energy of ~66 μJ/pulse, as measured prior to attenuation, was used for all experiments and corresponds to a ~50 μm beam diameter. The instrument was operated in negative ion MS/MS mode at 4 kV and utilized continuous laser raster sampling [34, 43–48] Plasma data were acquired in typewriter imaging mode using a 1-kHz laser repetition rate, 1-mm/s stage velocity, 100 hardware averages, and 100-μm vertical step size (resulting in 100-μm by 100-μm pixel sizes). Imaging data were acquired in typewriter imaging mode using a 1-kHz laser repetition rate, 1-mm/s stage velocity, 50 hardware averages, and 50-μm vertical step size (resulting in 50-μm by 50-μm pixel sizes). While pixels represent averages of spectra, multiple TOF/TOF events are indeed performed in each laser shot. For both the spotted analysis and the imaging analysis, an intensity filter was applied during acquisition to only record spectra above a desired intensity threshold. Following acquisition, spectral averages were manually exported using a region of interest selection tool from each manual spot and microspot. Instrument control and data acquisition utilized the SimulTOF Controller and data analysis was performed using the SimulTOF Viewer (SimulTOF Systems) as well as Microsoft Excel (Redmond, WA, USA). The quantitative RIF image was generated using in-house software developed using MATLAB (The MathWorks, Inc., Natick, MA, USA). External calibration was performed in both MS and MS/MS mode using RIF and RPT drug standards.

RIF plasma and IMS quantification experiments using multiple TOF/TOF events in a single laser shot were performed in a manner similar to that previously described [39, 49, 50]. Briefly, the instrument operates by first extracting the ions from the first source region of the instrument via pulsed extraction. As the precursor ions enter the first field-free drift (TOF-1) region of the instrument, they are separated by *m*/*z*. A precision timed ion selector (TIS, 500 FWHM resolution, 6-ns transition speed) located at the velocity focal distance is then used to sequentially isolate multiple precursor ions of interest of increasing *m*/*z*. This is performed by 'opening' and 'closing' the TIS multiple times within the same laser shot. Following isolation, the ions enter a collision cell (however, post-source decay [PSD] [51] using no collision gas was utilized for all experiments herein) and are then reaccelerated to 2 kV in the second source region. As with the TIS isolation, the second source region can be ramped multiple times within the same laser shot to reaccelerate ions from precursor ions of increasing *m*/*z*. Due to the rise and fall times of the power supplies and the ion transit times through the relevant devices, precursor ions must differ by at least 6%–7% in order to be successfully isolated and reaccelerated using this approach. As RIF and RPT differ only by 6.8% in mass, manual adjustment of the TIS and Source 2 settings was required to ensure proper isolation and reacceleration of each individual precursor ion (vide infra). Following reacceleration, the ion beam enters the TOF-2 region of the instrument where the fragment and remaining precursor ions are separated and travel through a two-stage ion mirror prior to impacting a multichannel plate detector (High Mass Bi-Polar TOF detector; Photonis, Sturbridge, MA, USA).

HPLC-MS/MS

High performance liquid chromatography-tandem mass spectrometry (HPLC-MS/MS) was used to validate the IMS quantification [32]. The dosed liver and a control liver were cut (~80 mg), homogenized in 10% methanol/water (~30 mg/mL), and analyzed similar to previously published methods [52, 53]. Stock solutions of RIF (0.466 mg/mL) and $^{13}C_1$,$^{2}H_1$-RIF (0.376 mg/mL) were used to spike calibration standards (2.58E-3 to 5.16E-1 μg RIF with 1.88E-1 μg $^{13}C_1$,$^{2}H_1$-RIF) into 150 μL of the control liver homogenate. Only the internal standard was spiked into 150 μL of the dosed tissue homogenates. All samples were diluted with methanol to a final volume of 800 μL and were centrifuged at 10,000 RPM for 10 min. The supernatants were separated by reversed phase liquid chromatography using a C18 column (30 × 2 mm, Luna 3 μm, 100 Å; Phenomenex, Torrance, CA, USA) and analyzed on a triple quadrupole MS/MS instrument (Agilent 6430). The solvents used for the HPLC separation were 0.1% formic acid in water (A) and methanol (B). The gradient was as follows: linearly decrease from 90% to 10% solvent A over 5 min, hold for 1 min, linearly increase to 90% solvent A in 1 min, and hold for 3 min. The transitions of *m*/*z* 821 to *m*/*z* 397 (RIF) and *m*/*z* 823 to *m*/*z* 399 ($^{13}C_1$,$^{2}H_1$-RIF) were monitored and the retention times were approximately 5.1 min. The concentration of RIF in liver as determined by HPLC-MS/MS was 23.2 μg/g.

Results

Multiple MS/MS Events in a Single Laser Shot

The TOF/TOF instrument used in these studies uniquely provides for the individual selection and reacceleration of multiple precursor ions in each laser shot. An example of this type of experiment is shown using RIF and RPT (Figure 1). Initially, the mass spectrum is reported as a function of the ion arrival time at the detector (Figure 1a). The mass spectrum can then be calibrated using either RIF or RPT as the precursor ion. In this instance, the lower molecular weight fragment ion (blue *m*/*z* 452) of the higher mass precursor ion (RPT, *m*/*z* 876) arrives at the detector before the lower mass precursor ion (RIF, *m*/*z* 821), viz.: the RIF precursor ion appears in the mass spectrum between the fragment and precursor ions of RPT. When fragment ion spectra overlap with one another in this manner, de novo interpretation of the spectrum is very challenging, and the

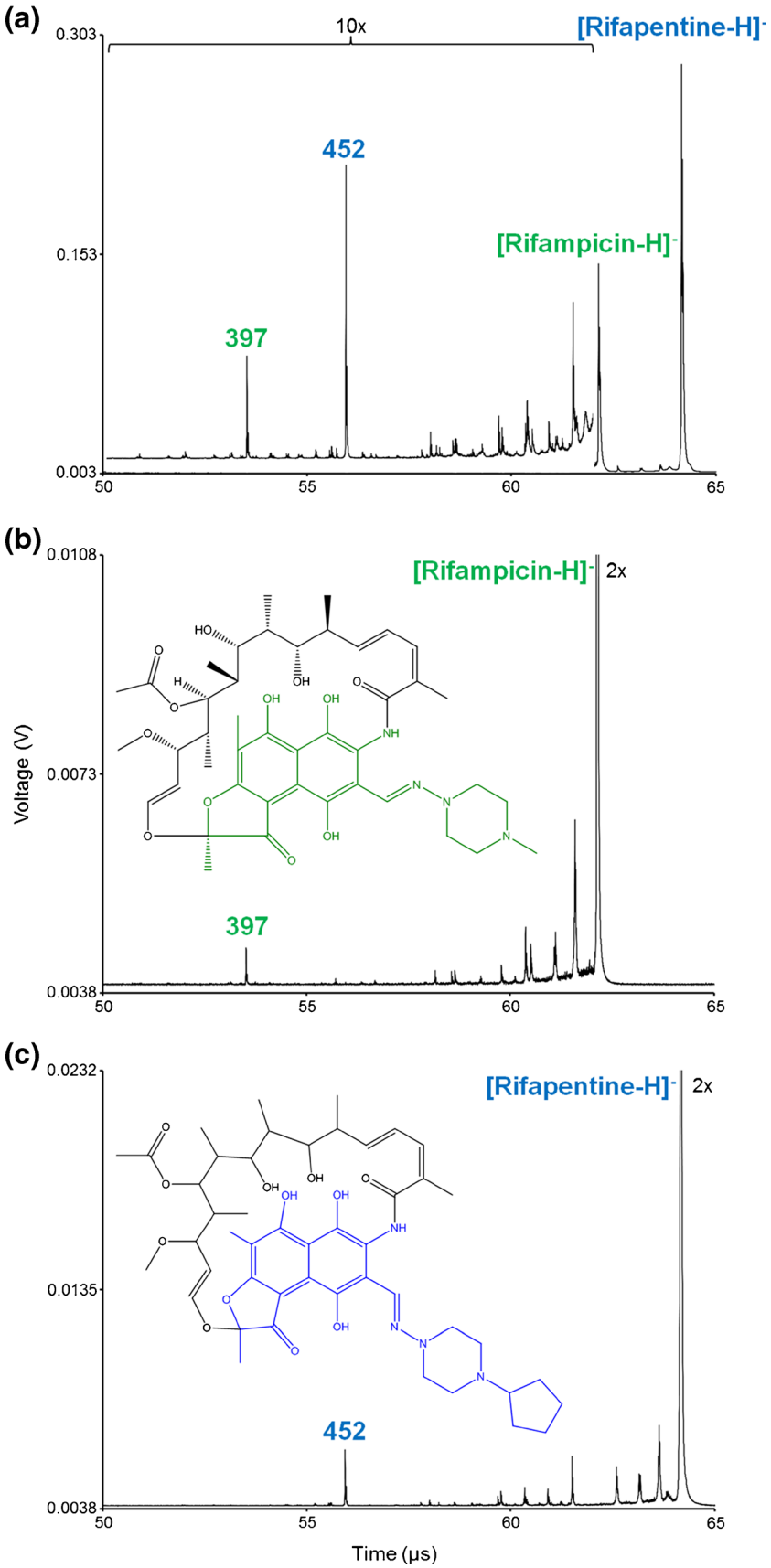

Figure 1. (**a**) RIF and RPT are each individually fragmented in a single laser shot. The MS/MS spectra of just (**b**) RIF and (**c**) RPT alone are used to ensure proper fragment ion mass assignment. The colored portions of the structure insets highlight the fragment ions of interest. Spectra represent an average of ~10,000 laser shots

user should have a priori knowledge of the fragmentation behaviors of the precursor ions of interest in order to ensure proper assignment of each fragment ion to the appropriate precursor ion. This is achieved by performing MS/MS experiments on each precursor ion individually (Figure 1b, c). This fragmentation fingerprint can then be used to accurately assign each fragment ion to the appropriate precursor ion in experiments that involve multiple ions selected for fragmentation. Once the proper precursor ion for each fragment ion has been identified, the correct *m/z* can be assigned based on the proper mass calibration.

RIF TOF/TOF Assay

We have recently reported the use of multiple TOF/TOF events in a single laser shot for improved quantification of manually spotted samples [39]. Briefly, this methodology uses one TOF/TOF event for an analyte and a second TOF/TOF event for an internal standard. This allows the intensity of the analyte to be referenced to the intensity of the internal standard in each laser shot even in instances where the two ions are quite disparate in *m/z*, such as in the case of RIF and RPT. In this instance, simply broadening the isolation window to ~56 Da to allow for the transmittance of both precursor ions would transmit an excess of chemical noise, resulting in a diminished signal-to-noise ratio that would compromise the limit of detection and lower limit of quantification, and mitigating the benefits of MS/MS specificity [39].

In applying this methodology to RIF quantification, this analysis was first performed using spotted MALDI samples. As RIF and RPT possess similar physical and chemical properties, the use of RPT as an internal standard represents an ideal test case for MALDI MS/MS quantification using multiple TOF/TOF events [54]. Working calibration (3.00–100.0 μM) and QC (50.0 μM) solutions of RIF included 50.0 μM RPT as an internal standard and a final concentration of 30% pooled human plasma containing K2EDTA as an anticoagulant. Each solution was premixed with THAP prior to manual spotting onto a gold-coated stainless steel MALDI target. Five sets of RIF/RPT spots were prepared and analyzed on the TOF/TOF platform. The data were acquired in imaging mode (data not shown) using an intensity filter set to only record a spectrum when at least two peaks reached 0.01 V in intensity. The TIS was set for a difference of 33 (TISB Delay Equation = 1882, TISB Pulse End Equation = 1915), resulting in pulse lengths of ~625 and ~640 ns for the TIS isolation events for RIF and RPT, respectively. This corresponds to ~3–4 Da isolation windows.The Source 2 Pulse End Slope was set to 1.003, resulting in ~115 ns and ~120 ns Source 2 pulse lengths for RIF and RPT, respectively. Following data acquisition, peak detection settings were optimized to detect both the ^{12}C and ^{13}C isotopes of the RIF and RPT fragment ions (default preset, minimum SNR: 1, max peak width: 3E-08 s, de-isotope width: 0.0001). Regions of interest were manually selected in the SimulTOF Viewer for each MALDI spot in order to generate an average spectrum. A peak list with corresponding peak areas was then exported to Excel for each spot where the ^{12}C and ^{13}C isotopes of each drug fragment were summed and quantitative analysis was performed.

RIF Quantification

MALDI MS/MS quantification without the use of an internal standard can be challenging. The relative standard deviations (RSDs) of the RIF analysis without normalization to the internal standard averaged 21.89% among the concentrations sampled, with all RSDs except one above 18% and as high as 28.23% ("Raw standard deviation" in Table 1). However, upon normalization to the RPT internal standard, the RSDs of RIF at every concentration dropped below 10% to an average of 5.08% ("Ratio standard deviation" in Table 1). This resulted in a greater than 4-fold improvement in RSD at most concentrations and provided for a dynamic range of nearly two orders of magnitude and a limit of quantification (LOQ) of 3.00 μM. This LOQ of ~2500 ng/mL is within the clinically-relevant therapeutic range following a single 10 mg/kg oral dose [55]. In addition to an improvement in precision, improvements in RIF linearity (Supplementary Figure 1) and accuracy (Table 2) were also observed upon normalization to RPT. As determined in the range of 3.00 to 100.0 μM, a least squares linear repression analysis showed an improvement in the correlation coefficient from $R^2 \approx 0.9881$ to $R^2 \approx 0.9992$ upon normalization (Supplementary Figure 1). Upon normalization, the average accuracy of the QC improved from 87.7% to 95.5%, with the accuracy for all QCs in the normalized data above 93% (Table 2). Additionally, the relative error as calculated using a $1/x^2$ weighted linear regression improved from an average of 14.4% to 8.2% upon normalization, resulting in an improvement in relative error at nearly every concentration (Table 2). Although not surprising that normalization to an internal standard improves accuracy, precision, and linearity, this work validates the use of multiple TOF/TOF events in a single laser shot for improved RIF quantification.

Table 1. Normalization to the RPT Internal Standard Improves Precision in RIF Quantification (n = 5)

Concentration (μM)	Average Raw (Abundance)	Average Ratio (Rifampicin/Rifapentine)	Raw Standard Deviation (%)	Ratio Standard Deviation (%)
3.00	564.94	0.0070465	27.48	9.45
7.00	1,323.86	0.014467	20.77	5.62
10.0	1,865.18	0.022131	28.23	6.86
30.0	6,610.27	0.071953	18.90	4.28
70.0	13,912.07	0.17251	21.80	2.40
100.0	23,958.21	0.25780	14.17	1.86

Table 2. Normalization to the RPT Internal Standard Improves Accuracy in RIF Quantification (n = 5)

Cocentration (μM)	Raw Relative Error (%)	Ratio Relative Error (%)
3.00	29.0	10.8
7.00	19.2	17.8
10.0	18.3	10.6
30.0	0.8	1.3
70.0	8.3	2.0
100.0	10.9	6.8
Concentration (μM)	Raw Accuracy (%)	Ratio Accuracy
50.0	87.7	95.5

Relative Error was Calculated Using $1/x^2$ Weighted Linear Regression. QC Accuracy is Reported as the Average of the Five Trials Using the Difference from 100% of the Absolute Value of the%error

Table 4. Normalization to the RPT Internal Standard Improves the Accuracy of the RIF Calibration Curve for IMS (n = 8 Microspots)

Cocentration (μM)	Raw Relative Error (%)	Ratio Relative Error (%)
8.00	82.7	4.42
12.00	56.22	6.09
16.00	41.42	14.74
20.00	33.33	4.44
24.00	27.72	1.80
Concentration (μM)	Raw Accuracy (%)	Ratio Accuracy
14.00	83.49	87.60

Relative Error was Calculated Using unweighted ($1/x^0$) Linear Regression. QC Accuracy is Reported as the Average of the 8 Microspots Using the Difference from 100% of the Absolute Value of the %Error

MALDI IMS Quantification

The absolute quantitative measurement of drug distributions throughout tissue microenvironments is an important area of pharmaceutical research. Recently, we have reported a quantitative IMS method for RIF in rabbit livers that uses an isotopically labeled internal standard for pixel-to-pixel quantification [32]. As discussed previously, an isotopically labeled internal standard may not be available in all instances and simply broadening the MS/MS isolation window to accommodate analyte and internal standard precursor ions of quite different *m/z* is not practical. As such, we have extended the use of multiple TOF/TOF events in a single laser shot to quantitative MALDI IMS.

In this analysis, a calibration curve of RIF (0–24.0 μM RIF with 20.0 μM RPT) and a QC solution (14.0 μM RIF with 20.0 μM rifapentine) were spotted onto a non-dosed liver tissue section. The internal standard was then deposited in a microspotted array with a spatial resolution of 1 mm across the tissue dosed in vivo. The THAP matrix was deposited onto the calibration standard and dosed tissue microspots. Eight different microspots were averaged at each concentration in order to generate the calibration curve on the non-dosed tissue section. Upon normalization to the internal standard, the relative standard deviation of the concentrations in the calibration curve improved from an average of 24.88% to an average of 15.22% (Table 3). The RSDs improved at each concentration, with no RSD above 18% following normalization. While linearity was diminished upon normalization (Supplementary Figure 2), RIF accuracy was once again dramatically improved upon normalization to the RPT internal standard (Table 4). Though QC accuracy only improved slightly, from 83.49% without normalization to 87.60% with normalization (all but one microspot above 86% upon normalization), unweighted relative error ($1/x^0$) markedly improved. Without normalization, the average relative error was 48.3%, with no error below 27% and as high as 83%. However, upon normalization, the average relative error of the calibration curve dropped to 6.29%, with no error above 15% and most below 6%. It should be noted that Table 3, Supplementary Figure 2, and Table 4 are calculated using the quantifiable range of the calibration curve (8.00–24.0 μM RIF as determined by an RSD cutoff of 20%).

The microspotted quantitative image of RIF shows differential distribution throughout the liver section (Figure 2a). The detected concentration of the drug within the blood vessels is lower, which is consistent with previous reports and is likely due to the drug binding to a blood protein such as albumin or α-1-acid glycoprotein (Figure 2b) [32, 56]. Heterogeneity within the tissue section may also be expected because of the known dynamic zonation of hepatic metabolism [57]. Novel to this type of microspot analysis is the ability to measure an absolute quantity of the drug at each microspot [32]. No RIF was detected in the microspots that landed off of the dosed tissue section (not pictured in Figure 2a), and these concentrations were not included in the reported IMS average concentration (Figure 2c). The concentration at each microspot was determined by first calculating the RIF concentration in femtomoles per microliter using the calibration curve from the non-dosed tissue section. The absolute amount of RIF in micrograms present at each microspot was then determined using this RIF concentration and the known volume of internal standard spotted using a robotic spotter (40 droplets total, each with a volume of 170 pL). Treating each tissue microspot as a cylinder and assuming a tissue density of 1.05 g/cm^3, a tissue thickness of 12 μm, and a microspot radius of 295 μm, the average amount of liver tissue at each microspot was determined to be 3.44E-6 g. By this, the absolute RIF

Table 3. Normalization to the RPT Internal Standard Improves the Precision of the RIF Calibration Curve for IMS (n = 8 Microspots)

Concentration (μM)	Average Raw (Abundance)	Average Ratio (Rifampicin/Rifapentine)	Raw Standard Deviation (%)	Ratio Standard Deviation (%)
8.00	163.71	0.2786	32.36	17.62
12.00	297.89	0.4720	28.23	13.69
16.00	440.81	0.6860	21.47	18.01
20.00	578.27	0.7822	19.72	11.02
24.00	717.54	0.8841	22.60	15.78

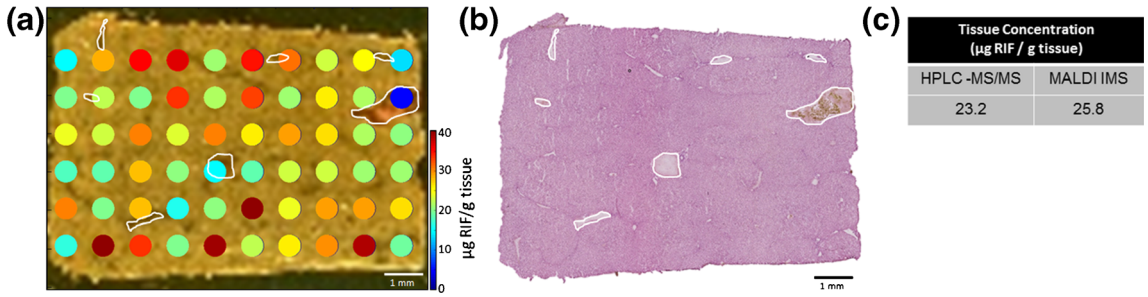

Tissue Concentration (µg RIF / g tissue)	
HPLC -MS/MS	MALDI IMS
23.2	25.8

Figure 2. (**a**) Quantitative MALDI IMS of RIF in rabbit liver at a spatial resolution of 1 mm shows diminished drug concentration in the blood vessels (outlined in white). (**b**) A serial section stained with hematoxylin and eosin allows facile visualization of the blood vessels. (**c**) MALDI IMS data and HPLC-MS/MS data are in agreement (10.6% difference)

concentration can be reported as micrograms of RIF per gram of tissue. Averaging the absolute concentration of RIF at each microspot across the tissue resulted in a value of 25.8 µg RIF/g tissue. A comparison of this concentration with that from HPLC-MS/MS analysis for a piece of the same liver tissue (23.2 µg RIF/g tissue) results in a percent difference of 10.6% (Figure 2c). However, in the HPLC-MS/MS results, the visualization of the drug within the tissue microenvironments is prohibited. Although the spatial resolution of the IMS experiment is fairly low here, differential localization of the drug across the tissue section is still observed.

Our previously reported quantitative imaging method, performed on the same tissue specimen using an ion trap platform, noted a concentration of 25.4 ± 4.9 µg RIF/g tissue as determined by HPLC-MS/MS and a concentration of 22.9 ± 2.6 µg RIF/g tissue as determined by MALDI IMS, a percent difference of 10.4% [32, 58]. In that work, it was determined that spotting the standards onto the tissue section followed by the matrix solution using the robotic spotter provided the most accurate concentrations for quantitative MALDI IMS (i.e., the same sample preparation methodology used here). Sequentially spotting the standards and matrix in this fashion prevents standard/matrix co-crystallization prior to the solutions reaching the tissue surface, which can result in disproportionately high ion intensity of the standard, and represents the most reproducible analyte extraction method [32]. Using the robotic spotter to deposit multiple droplets onto the tissue section also provides better penetration and mixing into the tissue section, more closely mimicking an in vivo analyte. Our previous results noted no statistically significant difference between RIF detected by MALDI IMS compared with HPLC-MS/MS, though there was a trend towards slightly lower drug concentrations determined by IMS compared with HPLC [32]. Those data included a MALDI IMS experimental precision of ~11%, suggesting that the variation between IMS and HPLC results observed here are likely within experimental errors. As the ion trap and TOF/TOF experiments are both in good agreement with one another and with respect to HPLC-MS/MS measurements, this experiment provides further confidence in our quantitative methodology by validating the analysis on a second instrument platform. Additionally, the TOF/TOF platform offers increased throughput compared with the ion trap platform and, due to the separation in time of the precursor ions in the TOF-1 region of the instrument, provides the ability to separate isomeric fragment ions, which may be useful in some experiments [39].

Conclusions

We have demonstrated the use of multiple TOF/TOF events in a single laser shot for RIF quantification. The approach involves the individual isolation and reacceleration of multiple precursor ions in a single laser shot, allowing for the intensity of the analyte ion to be referenced to that of the internal standard in every single laser shot. This methodology is applied to the accurate quantification of RIF in a complex environment of pooled human plasma, providing for significant improvements in accuracy, precision, and linearity, and allows for quantification within clinically-relevant therapeutic ranges. In general, the types of analytes and internal standards available for the experiment will dictate the applicability of this TOF/TOF approach. The availability of a structural analogue that differs sufficiently in molecular weight will allow multiple TOF/TOF events to be used for the discrete analysis of the analyte and internal standard separately in each laser shot, as has been shown here. The use of an isotopically labeled internal standard will preclude the use of multiple separate TOF/TOF events for the analyte and internal standard. However, in these instances the TOF/TOF window can be widened to accommodate both the analyte and internal standard, and multiple TOF/TOF events can then be used to analyze multiple analyte and internal standard pairs, effectively multiplexing the assay and improving throughput [39]. This methodology can be used in quantitative MALDI IMS to provide for microspot measures of absolute concentrations of in vivo dosed drug compounds in tissue sections. This pixel-to-pixel quantification approach provided accurate levels of local RIF concentrations in rabbit liver compared with HPLC-MS/MS. Additionally, the TOF/TOF quantification methodology detailed here is in good agreement with quantitative IMS studies previously performed on the same tissue specimen using an ion trap platform.

Acknowledgments

The authors acknowledge Marvin Vestal, Kevin Hayden, and George Mills at SimulTOF Systems for their instrument

support, Clifton E. Barry III, Laura E. Via, and Gwendolyn A. Marriner at the National Institutes of Health/National Institute of Allergy and Infectious Diseases for providing the rabbit livers and synthesizing the $^{13}C_1$,$^{2}H_1$-RIF standard, and Tina Tsui at the Vanderbilt University Mass Spectrometry Research Center for the development of the MATLAB quantitative imaging software. This work was sponsored by the National Institutes of Health/National Institute of General Medical Sciences under Award 5P41 GM103391-05 and, in part, by the Bill and Melinda Gates Foundation Accelerator grant N01 HD23342. B.M.P. was supported by the National Institutes of Health under Award T32 ES007028. C.W.C. acknowledges receipt of a fellowship from Aegis Sciences Corporation.

References

1. Caprioli, R.M., Farmer, T.B., Gile, J.: Molecular imaging of biological samples: localization of peptides and proteins using MALDI-TOF MS. Analytical Chemistry **69**, 4751–4760 (1997)
2. Norris, J.L., Caprioli, R.M.: Analysis of tissue specimens by matrix-assisted laser desorption/ionization imaging mass spectrometry in biological and clinical research. Chem. Rev. **113**(4), 2309–2342 (2013)
3. Castellino, S., Groseclose, M.R., Wagner, D.: MALDI imaging mass spectrometry: bridging biology and chemistry in drug development. Bioanalysis **3**(21), 2427–2441 (2011)
4. Takai, N., Tanaka, Y., Inazawa, K., Saji, H.: Quantitative analysis of pharmaceutical drug distribution in multiple organs by imaging mass spectrometry. Rapid Commun. Mass Spectrom. **26**(13), 1549–1556 (2012)
5. Lanshoeft, C., Stutz, G., Elbast, W., Wolf, T., Walles, M., Stoeckli, M., Picard, F., Kretz, O.: Analysis of small molecule antibody–drug conjugate catabolites in rat liver and tumor tissue by liquid extraction surface analysis micro-capillary liquid chromatography/tandem mass spectrometry. Rapid Commun. Mass Spectrom. **30**(7), 823–832 (2016)
6. Hopfgartner, G., Husser, C., Zell, M.: High-throughput quantification of drugs and their metabolies in biosamples by LC-MS/MS and CE-MS/MS: possibilities and limitations. Therapeu. Drug Monitoring **24**(1), 134–143 (2002)
7. Hopfgartner, G., Bourgogne, E.: Quantitative high-throughput analysis of drugs in biological matrices by mass spectrometry. Mass Spectrom. Rev. **22**, 195–214 (2003)
8. Maurer, H.H.: Multi-analyte procedures for screening for and quantification of drugs in blood, plasma, or serum by liquid chromatography-single stage or tandem mass spectrometry (LC-MS or LC-MS/MS) relevant to clinical and forensic toxicology. Clin. Biochem. **38**(4), 310–318 (2005)
9. Goodwin, R., Scullion, P., Macintyre, L., Watson, D., Pitt, A.: Use of a solvent-free dry matrix coating for quantitative matrix-assisted laser desorption ionization imaging of 4-bromophenyl-1,4-diazabicyclo(3.2.2)nonane-4-carboxylate in rat brain and quantitative analysis of the drug from laser microdissected tissue regions. Anal. Chem. **82**(9), 3868–3873 (2010)
10. Hankin, J.A., Murphy, R.C.: Relationship between MALDI IMS intensity and measured quantity of selected phospholipids in rat brain sections. Anal. Chem. **82**(20), 8476–8484 (2010)
11. Hattori, K., Kajimura, M., Hishiki, T., Nakanishi, T., Kubo, A., Nagahata, Y., Ohmura, M., Yachie-Kinoshita, A., Matsuura, T., Morikawa, T., Nakamura, T., Setou, M., Suematsu, M.: Paradoxical ATP elevation in ischemic penumbra revealed by quantitative imaging mass spectrometry. Antioxidants Redox Signaling **13**(8), 1157–1167 (2010)
12. Nilsson, A., Fehniger, T.E., Gustavsson, L., Andersson, M., Kenne, K., Marko-Varga, G., Andre, P.E.: Fine mapping the spatial distribution and concentration of unlabeled drugs within tissue micro-compartments using imaging mass spectrometry. PLoS One **5**(7), e11411 (2010)
13. Koeniger, S.L., Talaty, N., Luo, Y., Ready, D., Voorbach, M., Seifert, T., Cepa, S., Fagerland, J.A., Bouska, J., Buck, W., Johnson, R.W., Spanton, S.: A quantitation method for mass spectrometry imaging. Rapid Commun. Mass Spectrom. **25**(4), 503–510 (2011)
14. Lagarrigue, M., Lavigne, R., Tabet, E., Genet, V., Thome, J.-P., Rondel, K., Guevel, B., Multigner, L., Samson, M., Pineau, C.: Localization and in situ absolute quantification of chlordecone in the mouse liver by MALDI imaging. Anal. Chem. **86**(12), 5775–5783 (2014)
15. Fehniger, T., Végvári, A., Rezeli, M., Prikk, K., Ross, P., Dahlbäck, M., Edula, G., Sepper, R., Marko-Varga, G.: Direct demonstration of tissue uptake of an inhaled drug: proof-of-principle study using matrix-assisted laser desorption ionization mass spectrometry imaging. Anal. Chem. **83**(21), 8329–8336 (2011)
16. Groseclose, M.R., Castellino, S.: A mimetic tissue model for the quantification of drug distributions by MALDI imaging mass spectrometry. Anal. Chem. **85**(21), 10099–10106 (2013)
17. Jadoul, L., Longuespee, R., Noel, A., De Pauw, E.: A spiked tissue-based approach for quantification of phosphatidylcholines in brain section by MALDI mass spectrometry imaging. Anal. Bioanal. Chem. **407**(8), 2095–2106 (2015)
18. Hamm, G., Bonnel, D., Legouffe, R., Pamelard, F., Delbos, J.-M., Bouzom, F., Stauber, J.: Quantitative mass spectrometry imaging of propranolol and olanzapine using tissue extinction calculation as normalization factor. J. Proteom. **75**(16), 4952–4961 (2012)
19. Duncan, M.W.R., Hunsucker, H., Stephen, W.: Quantitative matrix-assisted laser desorption/ionization mass spectrometry. Briefings Funct Genom. Proteom. **7**, 355–370 (2008)
20. Bunch, J., Clench, M.R., Richards, D.S.: Determination of pharmaceutical compounds in skin by imaging matrix-assisted laser desorption/ionisation mass spectrometry. Rapid Commun. Mass Spectrom. **18**(24), 3051–3060 (2004)
21. Hsieh, Y., Casale, R., Fukuda, E., Chen, J.W., Knemeyer, I., Wingate, J., Morrison, R., Korfmacher, W.: Matrix-assisted laser desorption/ionization imaging mass spectrometry for direct measurement of clozapine in rat brain tissue. Rapid Commun. Mass Spectrom. **20**(6), 965–972 (2006)
22. Reich, R.F., Cudzilo, K., Levisky, J.A., Yost, R.A.: Quantitative MALDI-MS^n analysis of cocaine in the autopsied brain of a human cocaine user employing a wide isolation window and internal standards. J. Am. Soc. Mass Spectrom. **21**(4), 564–571 (2010)
23. Pirman, D.A., Yost, R.A.: Quantitative tandem mass spectrometric imaging of endogenous acetyl-L-carnitine from piglet brain tissue using an internal standard. Anal. Chem. **83**(22), 8575–8581 (2011)
24. Prideaux, B., Dartois, V., Staab, D., Weiner, D., Goh, A., Via, L., Barry, C., Stoeckli, M.: High-sensitivity MALDI-MRM-MS imaging of moxifloxacin distribution in tuberculosis-infected rabbit lungs and granulomatous lesions. Anal. Chem. **83**(6), 2112–2118 (2011)
25. Kallback, P., Shariatgorji, M., Nilsson, A., Andren, P.E.: Novel mass spectrometry imaging software assisting labeled normalization and quantitation of drugs and neuropeptides directly in tissue sections. J. Proteom. **75**(16), 4941–4951 (2012)
26. Prideaux, B., Stoeckli, M.: Mass spectrometry imaging for drug distribution studies. J. Proteom. **75**(16), 4999–5013 (2012)
27. Pirman, D.A., Reich, R.F., Kiss, A., Heeren, R.M.A., Yost, R.A.: Quantitative MALDI tandem mass spectrometric imaging of cocaine from brain tissue with a deuterated internal standard. Anal. Chem. **85**(2), 1081–1089 (2013)
28. Pirman, D.A., Kiss, A., Heeren, R.M.A., Yost, R.A.: Identifying tissue-specific signal variation in MALDI mass spectrometric imaging by use of an internal standard. Anal. Chem. **85**(2), 1090–1096 (2013)
29. Schulz, S., Gerhardt, D., Meyer, B., Seegel, M., Schubach, B., Hopf, C., Matheis, K.: DMSO-enhanced MALDI MS imaging with normalization against a deuterated standard for relative quantification of dasatinib in serial mouse pharmacology studies. Anal. Bioanal. Chem. **405**(29), 9467–9476 (2013)
30. Buck, A., Halbritter, S., Spaeth, C., Feuchtinger, A., Aichler, M., Zitzelsberger, H., Janssen, K.-P., Walch, A.: Distribution and quantification of irinotecan and its active metabolite SN-38 in colon cancer murine model systems using MALDI MSI. Anal. Bioanal. Chem. **407**(8), 2107–2116 (2015)
31. Porta, T., Lesur, A., Varesio, E., Hopfgartner, G.: Quantification in MALDI-MS imaging: what can we learn from MALDI-selected reaction monitoring and what can we expect for imaging? Anal. Bioanal. Chem. **407**(8), 2177–2187 (2015)
32. Chumbley, C.W., Reyzer, M.L., Allen, J.A., Marriner, G.A., Via, L.E., Barry III, C.E., Caprioli, R.M.: Absolute quantitative MALDI imaging mass spectrometry: a case of rifampicin in liver tissues. Anal. Chem. **88**(4), 2392–2398 (2016)
33. Duncan, M.W., Matanovic, G., Cerpa-Poljak, A.: Quantitative analysis of low molecular weight compounds of biological interest by matrix-assisted

laser desorption ionization. Rapid Commun. Mass Spectrom. **7**, 1090–1094 (1993)
34. Prentice, B.M., Chumbly, C.W., Caprioli, R.M.: High-speed MALDI TOF/TOF imaging mass spectrometry using continuous raster sampling. J. Mass Spectrom. **50**(4), 703–710 (2015)
35. Hatsis, P., Brombacher, S., Corr, J., Kovarik, P., Volmer, D.A.: Quantitative analysis of small pharmaceutical drugs using a high repetition rate laser matrix-assisted laser/desorption ionization source. Rapid Commun. Mass Spectrom. **17**(20), 2303–2309 (2003)
36. Sleno, L., Volmer, D.A.: Some fundamental and technical aspects of the quantitative analysis of pharmaceutical drugs by matrix-assisted laser desorption/ionization mass spectrometry. Rapid Commun. Mass Spectrom. **19**(14), 1928–1936 (2005)
37. Reich, R.F.: Quantitative imaging of cocaine and its metabolites in brain tissue by matrix-assisted laser desorption/ionization linear ion trap tandem mass spectrometry. Dissertation, University of Florida (2010)
38. Erickson, B.K., Jedrychowski, M.P., McAlister, G.C., Everley, R.A., Kunz, R., Gygi, S.P.: Evaluating multiplexed quantitative phosphopeptide analysis on a hybrid quadrupole mass filter/linear ion trap/orbitrap mass spectrometer. Anal. Chem. **87**(2), 1241–1249 (2015)
39. Prentice, B.M., Chumbley, C.W., Hachey, B.C., Norris, J.L., Caprioli, R.M.: Multiple time-of-flight/time-of-flight events in a single laser shot for improved matrix-assisted laser desorption/ionization tandem mass spectrometry quantification. Anal. Chem. 2016. doi:10.1021/acs.analchem.6b02821
40. Bartolucci, C., Cellai, L., Difilippo, P., Segre, A., Brufani, M., Filocamo, L., Bianco, A.D., Guiso, M., Brizzi, V., Benedetto, A., Dicaro, A., Elia, G.: Rifamycins as inhibitors of retroviral reverse-transcriptase from M-MuLV, RAV-2, and HIV-1. Farmaco **47**(11), 1367–1383 (1992)
41. Vijn, R.J.A., Henricus J., Green, R., Castelijns, A.M.: Synthesis of alkyl- and aryl-substituted pyridines from (α,β-unsaturated) imines or oximes and carbonyl compounds. Synthesis **6**, 573–578 (1994)
42. Brufani, M., Cellai, L., Bartolini, B., Medici, I., Lagrasta, B.M.: New drugs with anticholestatic activity. WO2009010555 A1, 22 Jan 2009
43. Simmons, D.A.: Improved MALDI-MS imaging performance using continuous laser rastering. Appl. Biosyst. Technical Note 1–5 (2008)
44. Hopfgartner, G., Varesio, E., Stoeckli, M.: Matrix-assisted laser desorption/ionization mass spectrometric imaging of complete rat sections using a triple quadrupole linear ion trap. Rapid Commun Mass Spectrom. **23**(6), 733–736 (2009)
45. Trim, P., Djidja, M.-C., Atkinson, S., Oakes, K., Cole, L., Anderson, D., Hart, P., Francese, S., Clench, M.: Introduction of a 20 kHz Nd:YVO4 laser into a hybrid quadrupole time-of-flight mass spectrometer for MALDI-MS imaging. Anal. Bioanal. Chem. **397**(8), 3409–3419 (2010)
46. Spraggins, J.M., Caprioli, R.M.: High-speed MALDI-TOF imaging mass spectrometry: rapid ion image acquisition and considerations for next generation instrumentation. J. Am. Soc. Mass Spectrom. **22**(6), 1022–1031 (2011)
47. Griffiths, R., Sarsby, J., Guggenheim, E., Race, A., Steven, R., Fear, J., Lalor, P., Bunch, J.: Formal lithium fixation improves direct analysis of lipids in tissue by mass spectrometry. Anal. Chem. **85**(15), 7146–7153 (2013)
48. Lanekoff, I., Burnum-Johnson, K., Thomas, M., Short, J., Carson, J.P., Cha, J., Dey, S.K., Yang, P., Prieto Conaway, M.C., Laskin, J.: High-speed tandem mass spectrometric in situ imaging by nanospray desorption electrospray ionization mass spectrometry. Anal. Chem. **85**(20), 9596–9603 (2013)
49. Vestal, M.L.: TOF-TOF with high resolution precursor selection and multiplexed MS-MS. US Patent 7,838,824 B2, 23 Nov 2010
50. Vestal, M.L.: Tandem time-of-flight mass spectrometry with simultaneous space and velocity focusing. US Patent 8,847,155 B2, 30 Sep 2014
51. Spengler, B.: Post-source decay analysis in matrix-assister laser desorption/ionization mass spectrometry of biomolecules. J. Mass Spectrom. **32**, 1019–1036 (1997)
52. Fang, P.F., Cai, H.L., Li, H.D., Zhu, R.H., Tan, Q.Y., Gao, W., Xu, P., Liu, Y.P., Zhang, W.Y., Chen, Y.C., Zhang, F.: Simultaneous determination of isoniazid, rifampicin, levofloxacin in mouse tissues and plasma by high performance liquid chromatography-tandem mass spectrometry. J. Chromatogra. B **878**(24), 2286–2291 (2010)
53. Chumbley, C.W., Reyzer, M.L., Allen, J.L., Marriner, G.A., Via, L.E., Barry III, C.E., Caprioli, R.M.: Absolute quantitative MALDI imaging mass spectrometry: a case of rifampicin in liver tissues. Anal. Chem. **88**(4), 2292–2398 (2016)
54. Parson, T.L., Marzinke, M.A., Hoang, T., Bliven-Sizemore, E., Weiner, M., Mac Kenzie, W.R., Dorman, S.E., Dooley, K.E.: Quantification of rifapentine, a potent antituberculosis drug, from dried blood spot samples using liquid chromatographic-tandem mass spectrometric analysis. Antimicrob. Agents Chemother. **58**(11), 6747–6757 (2014)
55. Srivastava, A., Waterhouse, D., Ardrey, A., Ward, S.A.: Quantification of rifampicin in human plasma and cerebrospinal fluid by a highly sensitive and rapid liquid chromatographic-tandem mass spectrometric method. J. Pharmaceut. Biomed.l Anal. **70**, 523–528 (2012)
56. Woo, J., Cheung, W., Chan, R., Chan, H.S., Cheng, A., Chan, K.: In vitro protein binding characteristics of isoniazid, rifampicin, and pyrazinamide to whole plasma, albumin, and alpha-1-acid glycoprotein. Clin. Biochem. **29**(2), 175–177 (1996)
57. Katz, N.R.: Metabolic heterogeneity of hepatocytes across the liver acinus. J. Nutri. **122**, 843–849 (1992)
58. Chumbley, C.W.: Absolute quantitative matrix-assisted laser desorption/ionization mass spectrometry and imaging mass spectrometry of pharmaceutical drugs from biological specimens. Vanderbilt University (2016)